2006

Refrigerant R410A Vaporisation Inside a Small Brazed Plate Heat Exchanger

Giovanni A. Longo
University of Padova

Andrea Gasparella
University of Padova

Refrigerant R410A Vaporisation Inside a Small Brazed Plate Heat Exchanger

Giovanni A. LONGO*, Andrea GASPARELLA

University of Padova, Department of Management and Engineering
Str.lla S.Nicola No.3, I-36100 Vicenza, ITALY
Phone: +39 0444 998726 Fax: +39 0444 998888 E-Mail: tony@gest.unipd.it

ABSTRACT

This paper presents the experimental heat transfer coefficients and pressure drop measured during refrigerant R410A vaporisation inside a small brazed plate heat exchanger: the effects of heat flux, refrigerant mass flux, saturation temperature and outlet conditions are investigated.
The experimental results are reported in terms of refrigerant side heat transfer coefficients and frictional pressure drop. The heat transfer coefficients show high sensitivity both to heat flux and outlet conditions and weak sensitivity to saturation temperature. The frictional pressure drop shows high sensitivity to refrigerant mass flux and weak sensitivity both to saturation temperature and outlet conditions.
The experimental heat transfer coefficients are also compared with two well-known correlations for nucleate pool boiling: a fair agreement is found.

1. INTRODUCTION

The phase-out of traditional chlorofluorocarbon (CFC) and hydrochlorofluorocarbon (HCFC) refrigerants involves the development and commercialisation of hydrofluorocarbon (HFC) refrigerants. HFC-134a is the substitute for CFC-12 in domestic refrigeration and mobile air conditioning, whereas HFC-407C and HFC-410A are the alternative for HCFC-22 in chillers and heat pumps. HFC-407C, a non azeotropic ternary mixture HFC-32/HFC-125/HFC-134a (23/25/52 wt%), is the equivalent pressure replacement which can be used not only in new equipment but also in exiting equipment. HFC-410A, a nearly azeotropic mixture HFC-32/HFC-125 (50/50% wt%), is the alternative for use in new equipment specifically designed for its high operating pressure.
Traditional gasket plate heat exchangers (PHE) have been used since the 1930s for liquid-to-liquid heat transfer, whereas in the 1970s the brazed plate heat exchangers (BPHE) have been developed for two-phase heat transfer, particularly as evaporators and condensers in chillers and heat pumps.
In open literature, it is possible to find several works on traditional PHE in single-phase liquid-to-liquid heat transfer, whereas limited data can be found on HFC refrigerant vaporisation and condensation inside BPHE. Yan and Lin (1999) and Yan *et al.* (1999) experimentally investigated the effects of mean vapour quality, mass flux, heat flux and saturation pressure on heat transfer and pressure drop during HFC-134a vaporisation and condensation inside a BPHE. They also presented empirical correlations for heat transfer coefficient and friction factor based on their experimental data. Hsieh and Lin (2002, 2003) reported experimental data on vaporisation heat transfer and pressure drop of HFC-410A in a BPHE. The effects of mean vapour quality, mass flux, heat flux and saturation pressure were evaluated and empirical correlations were proposed for heat transfer coefficient and friction factor. Han *et al.* (2003) presented experimental heat transfer coefficients and pressure drop measured during HFC-410A vaporisation inside a BPHE. The effects of mass flux, heat flux, saturation temperature and plate geometry (inclination angle of the corrugation) were evaluated and empirical correlations were proposed for Nusselt number and friction factor. Jokar *et al.* (2004) reported experimental data on HFC-134a condensation inside BPHE and proposed empirical correlations for heat transfer and pressure drop. Kuo *et al.* (2005) reported experimental data on HFC-410A condensation inside a PHE and proposed empirical correlations for heat transfer and pressure drop. Jassim *et al.* (2006) experimentally analysed the pressure drop in adiabatic two-phase flow of HFC-134a through a PHE with herringbone and bumpy corrugation: a two-phase pressure drop model based on the kinetic energy of the flow was also proposed.
This paper presents the experimental heat transfer coefficients and pressure drop measured during HFC-410A vaporisation inside a small BPHE: the effects of heat flux, refrigerant mass flux, saturation temperature and outlet conditions are investigated.

*Corresponding Author

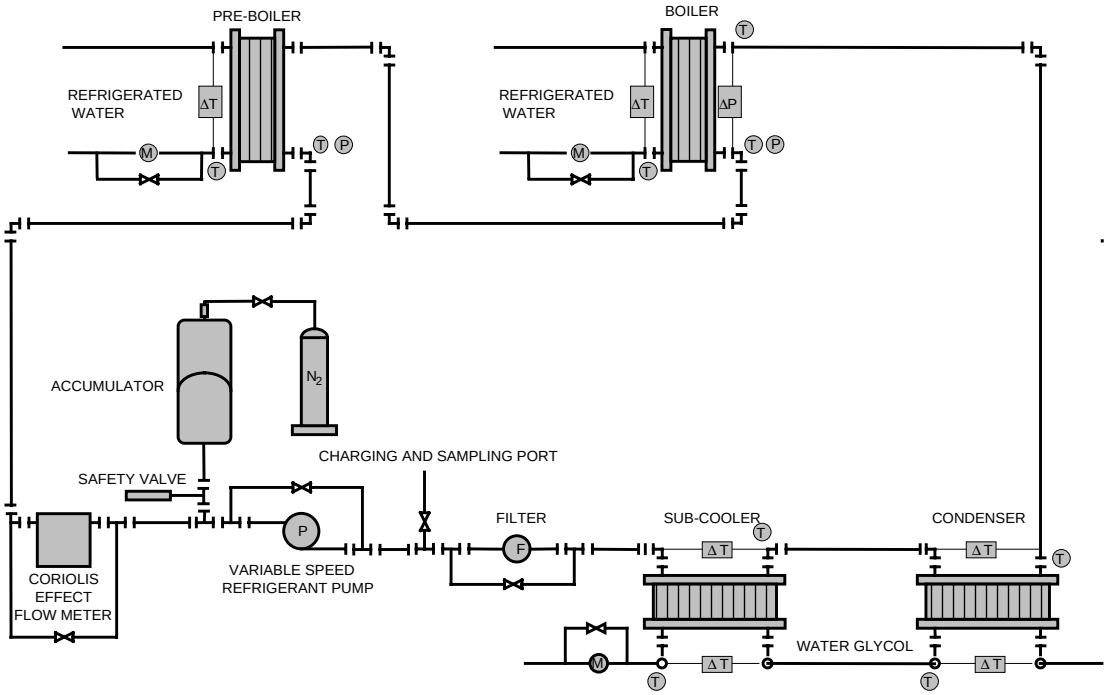

Figure 1: Schematic view of the experimental test rig

2. EXPERIMENTAL SET-UP AND PROCEDURES

The experimental facility, shown in figure 1, consists of a refrigerant loop, a water-glycol loop and a refrigerated water loop. In the first loop the refrigerant is pumped from the sub-cooler into the pre-boiler where it is partially evaporated to achieve the set quality at the boiler inlet. The refrigerant goes through the boiler where it is evaporated and eventually super-heated and then it comes back to the condenser and the sub-cooler. A variable speed volumetric pump varies the refrigerant flow rate, whereas a bladder accumulator connected to a nitrogen bottle and a pressure regulator controls the operating pressure in the refrigerant loop. The second loop is able to supply a water-glycol flow at a constant temperature in the range of -10 to 30°C with a stability within ±0.1 K used to feed the sub-cooler and the condenser, whereas the third loop supplies a refrigerated water flow at a constant temperature in the range of 3 to 30°C with a stability within ±0.1 K used to feed the boiler and the pre-boiler. The boiler is a BPHE consisting of 10 plates, 72 mm in width and 310 mm in length, which present a macro-scale herringbone corrugation with an inclination angle of 65° and a corrugation amplitude of 2 mm. Figure 2 and table 1 give the main geometrical characteristics of the BPHE tested.The temperatures of refrigerant and water at the inlet and outlet of the boiler and the pre-boiler are measured by T-type thermocouples (uncertainty within ±0.1 K), whereas water temperature drops through the boiler and the pre-boiler are measured by T-type thermopiles (uncertainty within ±0.05 K). The refrigerant pressures at the inlet of the boiler and the pre-boiler are measured by two absolute strain-gage pressure transducers (uncertainty within 0.075% f.s.), whereas the refrigerant pressure drop through the boiler is measured by a strain-gage differential pressure transducer (uncertainty within 0.075% f.s.). The refrigerant mass flow rate is measured by means of a Coriolis effect mass flow meter (uncertainty of 0.1% of the measured value), whereas the water flow rates through the boiler and the pre-boiler are measured by means of magnetic flow meters (uncertainty of 0.15% of the f.s.). All the measurements are scanned and recorded by a data logger linked to a PC: table 2 gives the main features of the different measuring devices in the experimental rig. Before starting each test the refrigerant is re-circulated through the circuit, the condenser and the sub-cooler are fed with water glycol at a constant temperature and the boiler and pre-boiler are fed with water at a constant temperature. The refrigerant pressure and vapour quality at the inlet of the boiler and the vapour quality or super-heating at the outlet of the boiler are controlled by adjusting the bladder accumulator, the volumetric pump, the flow rate and the temperature of the water glycol and the refrigerated water. Once temperature, pressure, flow rate and vapour quality steady state conditions are achieved at the boiler inlet and outlet both on refrigerant and water sides all the readings are collected for a set time and the average value during this time is computed for each parameter recorded. The experimental results are reported in terms of refrigerant side heat transfer coefficients and pressure drop.

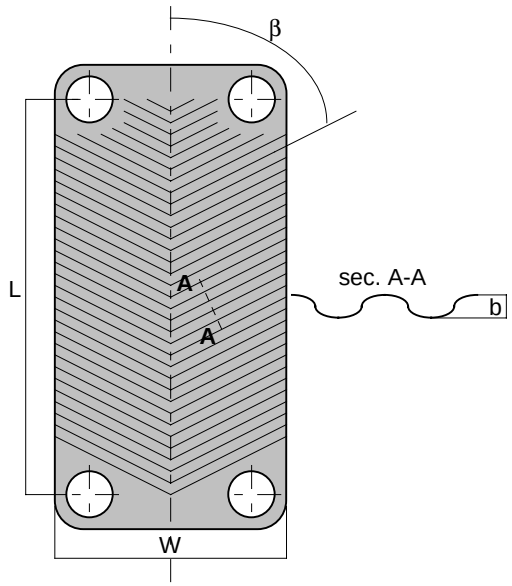

Figure 2: Schematic view of the plate

Table 1: Geometrical characteristics

Fluid flow plate length L (mm)	278.0
Plate width W(mm)	72.0
Area of the plate A(m^2)	0.020
Corrugation type	Herringbone
Angle of the corrugation β(°)	65
Corrugation amplitude b(mm)	2.0
Plate roughness R_a(μm)	0.4
Plate roughness R_p(μm)	1.0
Number of plates	10
Channels on refrigerant side	4
Channels on water side	5

3. DATA REDUCTION

3.1 Heat Transfer

The overall heat transfer coefficient in the boiler U is equal to the ratio between the heat flow rate Q, the nominal heat transfer area S and the logarithmic mean temperature difference ΔT_{ln}.

$$U = Q / (S\,\Delta T_{ln}) \quad (1)$$

The heat flow rate is derived from a thermal balance on the water side of the boiler:

$$Q = m_w\, c_{pw}\, |\Delta T_w| \quad (2)$$

where m_w is the water flow rate, c_{pw} the water specific heat capacity and $|\Delta T_w|$ the absolute value of the temperature variation on the water side of the boiler. The nominal heat transfer area of the boiler

$$S = N\,A \quad (3)$$

is equal to the nominal projected area $A = L \times W$ of the single plate multiplied by the number N of the effective elements in heat transfer, as suggested by Shah and Focke (1988).

Table 2: Specification of the different measuring devices

Devices	**Type**	**Uncertainty**	***Range***
Thermometers	- T-type thermocouples	0.1 K	-20 ÷ 80°C
Differential thermometers	- T-type thermopiles	0.05 K	-20 ÷ 80°C
Abs. pressure transducers	- Strain-gage	0.075% f.s.	0 ÷ 2.0 Mpa
Diff. pressure transducers	- Strain-gage	0.075% f.s.	0 ÷ 0.3 Mpa
Refrigerant flow meters	- Coriolis effect	0.1%	0 ÷ 300 kg/h
Water flow meters	- Magnetic	0.15%	100 ÷ 1200 l/h

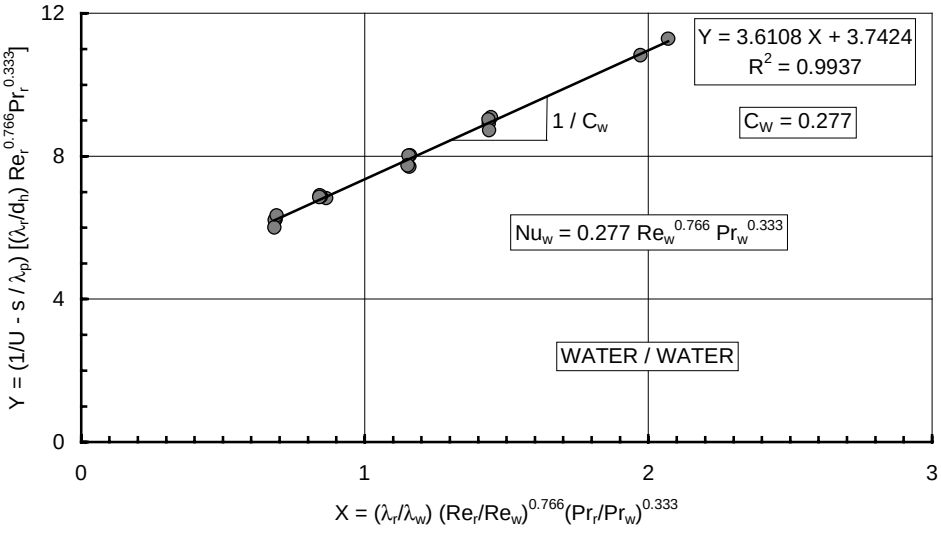

Figure 3: Modified Wilson plot results for calibration of water side heat transfer coefficient

The logarithmic mean temperature difference in the boiler is equal to

$$\Delta T_{ln} = [(T_{wo} - T_{wi}) / \ln [(T_{sat} - T_{wo})/(T_{sat} - T_{wi})] \quad (4)$$

where T_{sat} is the saturation temperature (dew point) of the refrigerant derived from the average pressure measured on refrigerant side and T_{wi} and T_{wo} the water temperatures at the inlet and the outlet of the boiler. The average heat transfer coefficient on the refrigerant side of the boiler h_r is derived from the global heat transfer coefficient U:

$$h_r = (1 / U - s / \lambda_p - 1 / h_w)^{-1} \quad (5)$$

by computing the water side heat transfer coefficient h_w using a modified Wilson plot technique. A specific set of experimental water to water tests is carried out on the boiler to determine the calibration correlation for heat transfer on the water side, in accordance with Muley and Manglick (1999). This modification of the classical Wilson plot technique incorporates an account of variable fluid property effects: figure 3 shows the water to water data plotted on the co-ordinates

$$X = (\lambda_r/\lambda_w) (Re_r/Re_w)^{0.766}(Pr_r/Pr_w)^{0.333} \quad (6)$$

$$Y = (1/U - s / \lambda_p) [(\lambda_r/d_h) Re_r^{0.766} Pr_r^{0.333}] \quad (7)$$

where subscripts r and w refer to the refrigerant and water side of the boiler respectively. The slope of the plot gives the constant in the calibration correlation, a power-law type, for heat transfer coefficients on the water side. The exponent on Reynolds number n = 0.766 results from a best fitting procedure on the experimental data. The calibration correlation for water side heat transfer coefficient results:

$$h_w = 0.277 (\lambda_w / d_h) Re_w^{0.766} Pr_w^{0.333} \quad (8)$$

The refrigerant vapour quality at the boiler inlet and outlet x_i and x_o are computed starting from the refrigerant temperature $T_{pb.i}$ and pressure $p_{pb.i}$ at the inlet of the pre-boiler (sub-cooled liquid condition) considering the heat flow rate exchanged in the pre-boiler and in the boiler Q_{pb} and Q and the pressure at the inlet and outlet p_i and p_o of the boiler as follows:

$$x_i = f(J_i, p_i) \quad (9)$$

$$x_o = f(J_o, p_o) \quad (10)$$

$$J_i = J_{pb.i} (T_{pb.i}, p_{pb.i}) + Q_{pb} / m_r \quad (11)$$

$$J_o = J_i + Q / m_r \quad (12)$$

$$Q_{pb} = m_{pb.w}\, c_{pw}\, |\Delta T_{pb.w}| \quad (13)$$

where J is the specific enthalpy of the refrigerant, m_r the refrigerant mass flow rate, $m_{pb.w}$ the water flow rate and $|\Delta T_{pb.w}|$ the absolute value of the temperature variation on the water side of the pre-boiler.
The refrigerant properties are evaluated by Refprop 7.0 (NIST (2002)).

3.2 Pressure drop

The frictional pressure drop on refrigerant side Δp_f is computed by subtracting the momentum pressure drop Δp_a, the gravity pressure drop Δp_g and the manifolds and ports pressure drops Δp_c from the total pressure drop measured Δp_t:

$$\Delta p_f = \Delta p_t - \Delta p_a - \Delta p_g - \Delta p_c \quad (14)$$

The momentum and gravity pressure drops are estimated by the homogeneous model for two-phase flow as follows:

$$\Delta p_a = G^2 (v_G - v_L)\, \Delta x \quad (15)$$

$$\Delta p_g = g\, L / v_m \quad (16)$$

where v_L and v_G are the specific volume of liquid and vapour phase, whereas v_m is the specific volume of the vapour-liquid mixture in the homogeneous model. The pressure drops in the inlet and outlet manifolds and ports are empirically estimated, in accordance with Shah and Focke (1988):

$$\Delta p_c = 1.5 \left(u_c^{\,2} / 2 v_m \right) \quad (17)$$

where u_c is the mean flow velocity calculated by the homogeneous model.

4. ANALYSIS OF THE RESULTS

A set of 84 vaporisation tests with HFC-410A refrigerant up-flow and water down-flow are carried out at four different saturation temperatures (5, 10, 15 and 20°C) and four different boiler outlet conditions (vapour quality around 0.80 and 1.00, vapour super-heating around 5 and 10°C). Table 3 gives the main operating conditions in the boiler under experimental tests: refrigerant saturation temperature T_{sat} and pressure p_{sat}, inlet and outlet refrigerant vapour quality x_i and x_o, outlet refrigerant super-heating ΔT_{sup}, mass flux on refrigerant side G_r and water side G_w, heat flux q. A detailed error analysis performed in accordance with Kline and McClintock (1953) indicates an overall uncertainty within ±12% for the refrigerant heat transfer coefficient measurement and within ±7% for the refrigerant pressure drop measurement.

4.1 Heat Transfer

Figure 4 shows the average heat transfer coefficients on the refrigerant side against heat flux for different saturation temperatures (5, 10 and 20°C) and different boiler outlet conditions (vapour quality around 0.80 and 1.00, vapour super-heating around 5 and 10°C). The heat transfer coefficients show high sensitivity to heat flux and outlet condition and weak sensitivity to saturation temperature. The saturated boiling heat transfer coefficients with an outlet vapour quality around 0.80 are 5% higher than the saturated boiling heat transfer coefficients with an outlet vapour quality around 1.00, 20% higher than the heat transfer coefficients with 5°C of outlet vapour super-heating and 40% higher than the heat transfer coefficients with 10°C of outlet vapour super-heating. The weak decrease of the heat transfer coefficients with outlet vapour quality is probably due to dryout inception in the upper part of the boiler, whereas the marked decrease of the heat transfer coefficient with vapour super-heating is due to the increase in the super-heating portion of the heat transfer area which is affected by gas single phase heat transfer coefficients.

Table 3: Operating conditions during experimental tests

Runs	T_{sat}(°C)	p_{sat}(MPa)	x_i	x_o	ΔT_{sup}(°C)	G_r(kg/m^{2}s)	G_w(kg/m^{2}s)	q(kW/m^2)
85	4.8–20.3	0.93–1.46	0.20-0.35	0.79–1.00	5.1–10.6	15.5–40.1	53.4–190.5	5.9–26.1

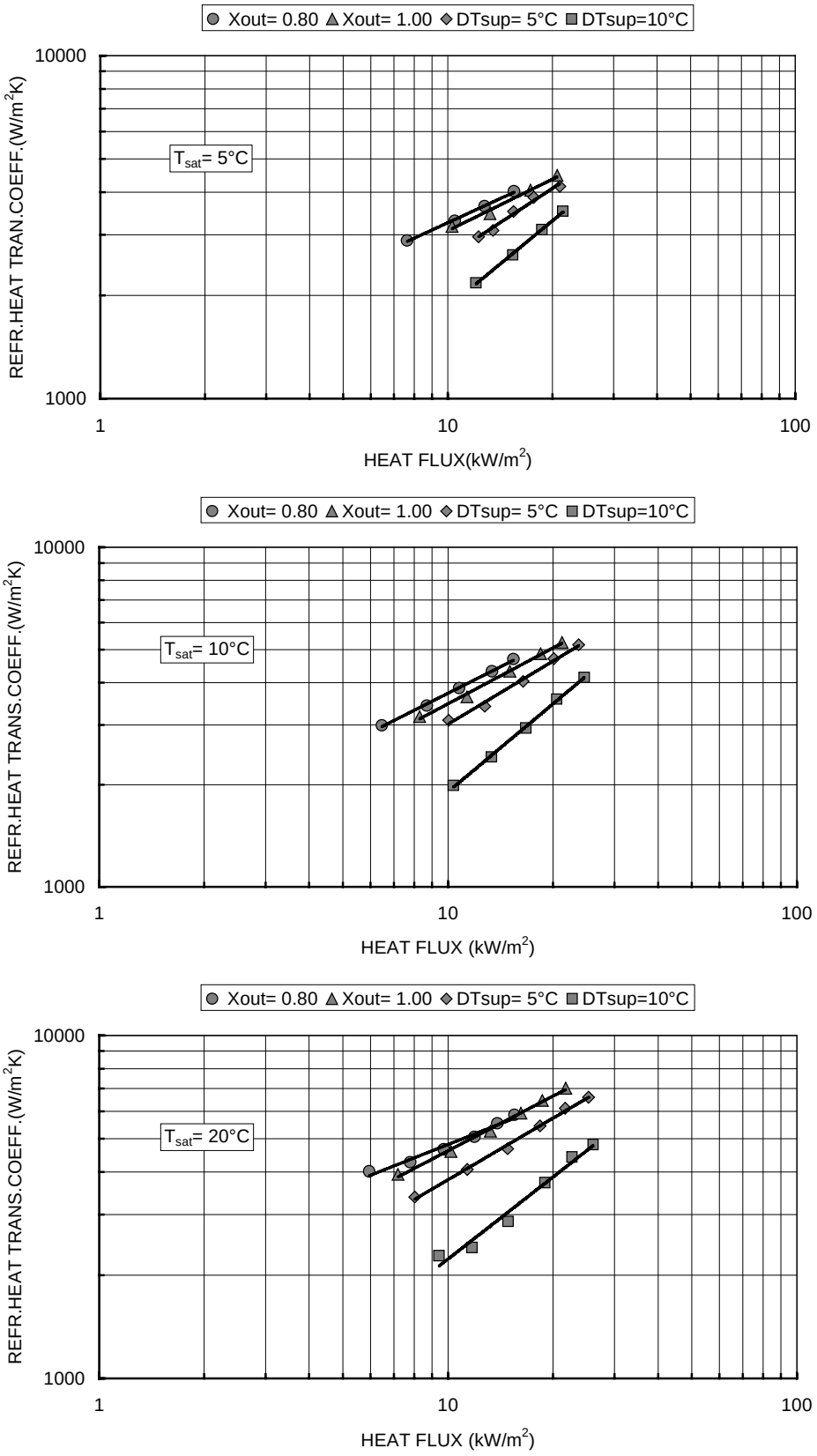

Figure 4: Average heat transfer coefficient on refrigerant side vs. heat flux for three different saturation temperatures

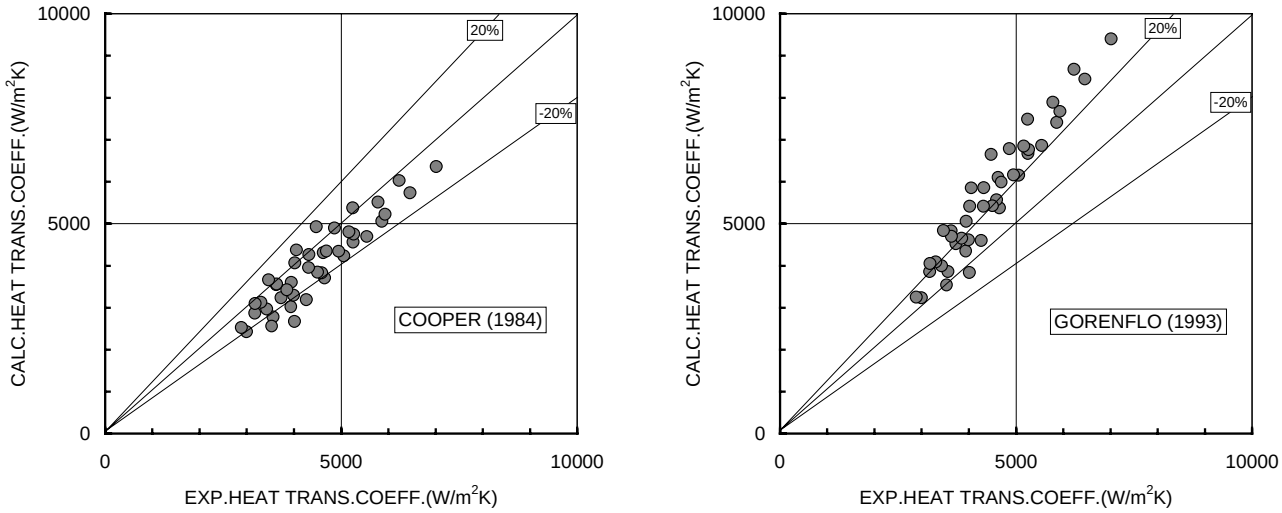

Figure 5: Comparison with Cooper (1984) and Gorenflo (1993) equations

The correlation between the saturated boiling heat transfer coefficients and heat flux is well represented by a power-law function with an exponent between 0.5-0.6.

The saturated boiling experimental heat transfer coefficients are compared with two well-known correlations for nucleate pool boiling: Cooper (1984) and Gorenflo (1993) equations. Figure 5 shows the comparison between saturated boiling experimental data and nucleate pool boiling correlations: the mean absolute percentage deviations are 11.4% and 25.5% for Cooper (1984) and Gorenflo (1993) equations respectively. The fair agreement between experimental and calculated data seems to confirm that nucleate boiling controls the present vaporisation data.

4.2 Pressure drop

Figure 6 shows the refrigerant side frictional pressure drop against the refrigerant mass flux for different saturation temperatures (5, 10, 15 and 20°C) and different boiler outlet conditions (vapour quality around 0.80 and 1.00, vapour super-heating around 5 and 10°C). The frictional pressure drop shows high sensitivity to refrigerant mass flux and weak sensitivity to saturation temperature and outlet conditions. The correlation between frictional pressure drop and refrigerant mass flux is well represented by a quadratic-law function.

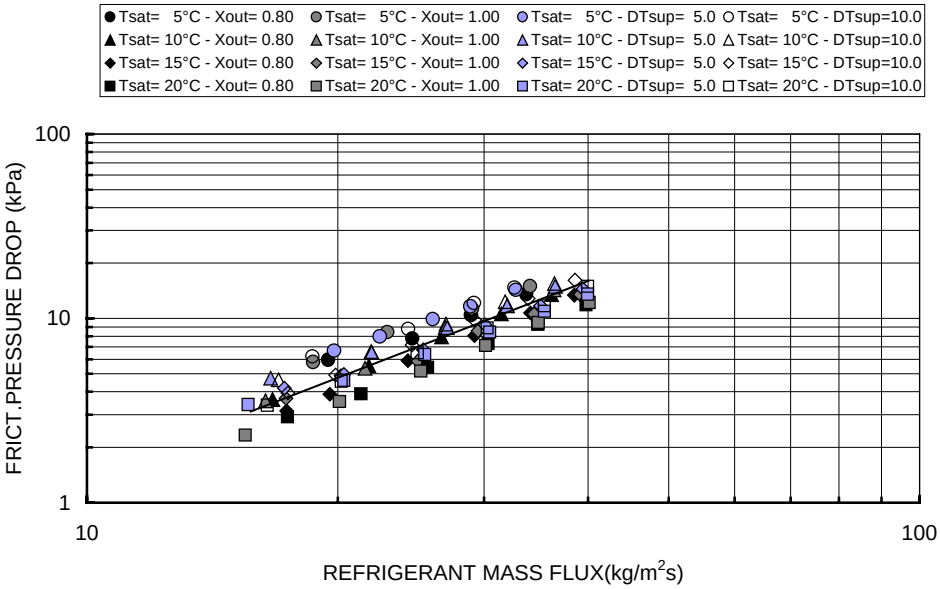

Figure 6: Frictional pressure drop on refrigerant side vs. refrigerant mass flux

5. CONCLUSIONS

This paper investigates the effect of heat flux, refrigerant mass flux, saturation temperature and outlet conditions on heat transfer and pressure drop during HFC-410A vaporisation inside a small brazed plate heat exchanger.
The heat transfer coefficients show great sensitivity both to heat flux and outlet conditions and negligible sensitivity to saturation temperature. The frictional pressure drop shows high sensitivity to refrigerant mass flux and weak sensitivity both to saturation temperature and outlet conditions.
The correlation between saturated boiling heat transfer coefficients and heat flux is well represented by a power-law function with an exponent around 0.5-0.6, whereas the frictional pressure drop is correlated to the refrigerant mass flux by a quadratic-law function.
Cooper 1984 and Gorenflo 1993 correlations reproduce saturated boiling experimental heat transfer coefficients with a mean absolute percentage deviation around 11.4 and 25.5% respectively: this fair agreement seems to confirm that nucleate boiling controls present vaporisation data.

REFERENCES

Cooper, M.G., 1984, Heat flows rates in saturated pool boiling – A wide ranging examination using reduced properties, *Advanced in Heat Transfer*, Academic Press, Orlando, Florida, 157-239.

Gorenflo, D., 1993, Pool boiling, *VDI Heat Atlas*, Dusseldorf, Germany, Ha1-25.

Han, D.H., Lee, K.J., Kim, Y.H., 2003, Experiments on the characteristics of evaporation of R410A in brazed plate heat exchangers with different geometric configurations, *Applied Thermal Eng*., 23, 1209-1225.

Hsieh, Y.Y., Lin, T.F., 2002, Saturated flow boiling heat transfer and pressure drop of refrigerant R410A in a vertical plate heat exchanger, *Int. J. Heat Mass Transfer*, 45, 1033-1044.

Hsieh, Y.Y., Lin, T.F., 2003, Evaporation heat transfer and pressure drop of refrigerant R410A in a vertical plate heat exchanger, *ASME J. Heat Transfer*, 125, 852-857.

Jassim, E.W., Newell ,T.A., Chato, J.C., 2006, Refrigerant pressure drop in chevron and bumpy style flat plate heat exchangers, *Exp. Therm. Fluid Science*, 30, 213-222.

Jokar, A., Eckels, S.J., Onsi, M.H., Gielda, T.P., 2004, Condensation heat transfer and pressure drop of brazed plate heat exchangers using refrigerant R134a, *J. Enhanced Heat Transfer*, 11, 161-182.

Kline, S.J., McClintock, F.A., 1953, Describing uncertainties in single-sample experiments, *Mech.Eng.*, 75, 3-8.

Kuo, W.S., Lie, Y.M., Hsieh, Y.Y., Lin, T.F., 2005, Condensation heat transfer and pressure drop of refrigerant R410A flow in a vertical plate heat exchanger, *Int. J. Heat Mass Transfer*, 48, 5205-5220

Muley, A., Manglik, R.M., 1999, Experimental study of turbulent flow heat transfer and pressure drop in a plate heat exchanger with chevron plates, *ASME J. Heat Transfer*, 121, 110-121.

NIST, 2002, Refrigerant properties computer code, REFPROP 7.0.

Shah, R.K., Focke, W.W., 1988, Plate heat exchangers and their design theory, Heat Transfer Equipment Design, Hemisphere, Washington, 227-254.

Thonon, B., Vidil, R., Marvillet, C., 1995, Recent research and developments in plate heat exchangers, J. *Enhanced Heat Transfer*, 2, 149-155.

Yan, Y.Y., Lio, H.C., Lin, T.F., 1999, Condensation heat transfer and pressure drop of refrigerant R134a in a plate heat exchanger, *Int. J. Heat Mass Transfer*, 42, 993-1006.

Yan, Y.Y., Lin, T.F., 1999, Evaporation heat transfer and pressure drop of refrigerant R134a in a plate heat exchanger, *ASME J. Heat Transfer*, 121, 118-127.